# Evaluation of topography site effect in slope stability under dynamic loading

Hieu Toan Nguyen, Jean-Alain Fleurisson, Roger Cojean

# Evaluation of topography site effect in slope stability under dynamic loading

**H.T. Nguyen[1], J.-A. Fleurisson[1], R. Cojean[1]**

[1] Geosciences and Geoengineering Research Department, Mines ParisTech, France

**Abstract.** The slope topography site effect is a phenomenon in which the seismic ground motion is amplified at the crest of the slope. This effect can damage structures and can even cause slope instabilities. The aim of this study is to explore the impact of slope geomorphology parameters on topographic site effects. A dimensionless factor, the ratio of the slope height to the seismic wavelength is identified as a critical parameter. Numerical simulations resulting in the seismic response of a uniform slope in an elastic material to excitation of vertically propagating SV waves, allowed defining the effects of these parameters to amplification factors and extension of the affected zones. In civil engineering, the knowledge of zones which will experience amplified excitation is important and essential for the structural design. In particular, the vicinity of the crest is a zone frequently affected by strong amplifications, and in some cases, earthquake-induced landslides may occur. For this reason, graphs derived from the results of numerous numerical analyses, can be useful to predicting the maximum amplification factors, the area as well as the dimension of the amplified zone in the vicinity of the crest.

*Keywords: site effect, dimensionless frequency, slope instability, amplification, earthquake*

## 1 INTRODUCTION

Many macroseismic observations throughout the world – France (Lambesc, 1909), Italy (Irpinia, 1980), California, USA (1987 and 1989) – showed that the seismic motion is amplified at the crest of slopes. This phenomenon, called topographic site effect, is the cause of the spatial, spectral and temporal modifications of the vibration signal characteristics. Topographic site effect is mainly caused by the interference of the incident waves and the ones reflected along the free surface. The interference of these waves gives an amplification of the seismic motion in the vicinity of the crest and a de-amplification near the toe of the slope (Bourdeau, 2005; Vanbrabant, 1998) (Figure 1). For this reason, a rolling topography may aggravate the impact of an earthquake, which can lead to structural damages and even to slope instabilities.

The impact of site effect is already specified in the French seismic code PS92 (applicable until 31st October 2012) and more recently in European EC-8 (Eurocode 8, 2005). However, only the slope morphology is considered in these regulations. Other factors such as the geological and the seismic characteristics of the slope and the characteristics of the excitation signal are not considered. Nevertheless, they have an important influence on the amplitude of the site effect and the dimension of the affected zone. In 1993 Dakoulas proposed a new parameter ($\eta$) named "dimensionless frequency" (Dakoulas, 1993). It combines the various involved parameters to a unique parameter which can therefore simply and effectively represent site effects. However it has not received much attention in scientific works. Some authors used it in specific case studies, but there is not yet any research works specifically on the usefulness of this parameter. For this reason, this paper focuses on the potential role of the dimensionless frequency in evaluating and predicting the site effects in general, and the topographic site effects in particular.
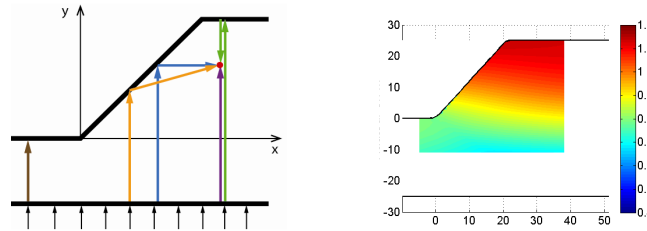
**Figure 1.**    Schematic illustration of topographic site effect mechanism and the horizontal acceleration amplification factor of a slope model in a uniform elastic material

## 2    METHODOLOGY OUTLINE

Numerical analyses were performed by finite difference method using Flac 2D (Itasca). In order to limit the amount of variables related to the geomorphologic context, the studied model contains only one uniform slope and the material is considered as homogeneous and elastic. The width and the height of the grid, according to the slope height (H), are set respectively at $20H+2H/\tan\alpha$ and $H+20m$ (Figure 3), in order to reduce artificial waves resulting from the reflection of the incident signal on the model boundaries into the study zone.

### 2.1    Mesh size

Mesh size of the slope model is set in order to correctly ensure the transmission of the seismic waves. According to Flac 2D user guide, this condition is guaranteed when equation (1) is satisfied: $\Delta l$ denotes the maximum size of a mesh element, $\lambda$ is the wavelength of the excitation seismic signal, and N value must be greater than 10. Then, for each case study, depending on the characteristic of the incident seismic wave that will be applied to the model, the mesh size is calculated so that expression (1) is always satisfied. For all the numerical simulations performed in this study, the value of N is chosen between 30 and 100. When the value of N is high, the numerical result error is small (Figure 2) but the computation time is long.

$$\Delta l \le \frac{\lambda}{N}$$

(1)
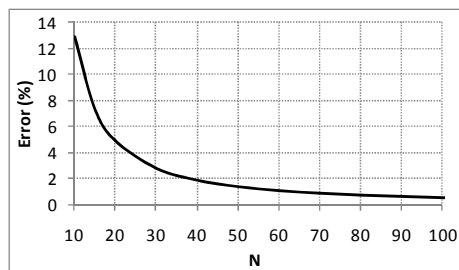


**Figure 2.**    Numerical result error according to the value of N

### 2.2    Boundary conditions

For the purpose of eliminating boundary effects and reflections of seismic wave on the lateral borders of the model, boundary conditions simulating the free field are applied to both vertical limits of the model. To prevent any additional reflection of the reflected waves going down from the free surface towards the substratum, an absorbing boundary condition named "quiet boundary" is applied to the model base as presented in Figure 3.

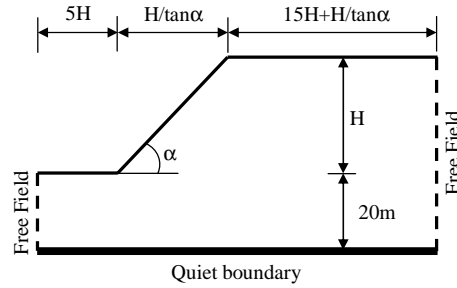**Figure 3.**    Size and boundary conditions of the slope model used in the numerical simulations

## 2.3  Seismic wave excitation

A SV wave is applied to the model base. The incident signal is an artificial mono-frequency wave in the form of a sinusoidal wave, with a Peak Ground Acceleration (PGA) of 0.4g (m/s²) and a frequency ranging from 0.5Hz to 10Hz.

## 2.4  Interpretation criteria

In this paper, the method of site/reference proposed by Borcherdt (Borcherdt, 1970) is used to evaluate the site effect. The three main criteria considered in the interpretation of the site effect are: the amplification factors, the proportion in area between the amplified zone and the study region, and the dimension of the amplified zone in the surroundings of the crest.

The first main interpretation criterion, the amplification factor, includes two sub criterions: the horizontal amplification (Ax) and the vertical amplification (Ay). Both are determined by the ratio between the maximal horizontal or vertical acceleration, calculated in the whole slope during the whole duration of the excitation, and the maximal horizontal acceleration calculated in a site of reference (horizontal bedrock in free field conditions). In homogeneous material, the measured value of such site of reference is always equal to twice the PGA of the incident wave. For Ax, if the calculated value (equation(2)) is greater than 1.0, amplification occurs, and on the opposite, it is a de-amplification. Even if the excitation source (SV wave) does not contain any vertical component, research works (Ashford et al., 1997),(Bouckovalas and Papadimitriou, 2005; Bouckovalas and Papadimitriou, 2006) showed that vertical component is also generated in some points within the model by the irregular topography. The value of the horizontal amplification is determined by expression(3). A point in the model is called "amplified" when Ay value calculated at this point is greater than zero.

$$Ax = \frac{xacc_{max}}{2PGA}$$

(2)

$$Ay = \frac{yacc_{max}}{2PGA}$$

(3)

The second main interpretation criterion has also two sub criterions. They are the proportion of the total amplified zone area ($pS_A$) and the proportion of the amplified zone area along the free surface ($pS_{AS}$). The calculated formulas are presented in equations (4) and (5).

$$pS_A = \frac{S_A}{S_T} \times 100$$

(4)

$$pS_{AS} = \frac{S_{AS}}{S_T} \times 100$$

(5)

$S_T$: the area of the studied region as the parallelogram limited by the part of the free surface corresponding to the slope and the dash dot line. The height and the length of this zone are respectively H and 2H.

$S_A$: the total amplified zone area. This area is the union of all the zones (in the studied region $S_T$) which are amplified during seismic excitation. For example, in Figure 4, the numbered zones were amplified at different time, and $S_A$ is the union of area of these four zones.

$S_{AS}$: the part of the total amplified zone area but located only along the free surface (in the studied region $S_T$). It is the union of area of three zones numbering 1, 2 and 3 in Figure 4.

The last criterion is the dimension of the horizontal amplification zone in the surroundings of the crest. This dimension is represented by two values: height (Hx) and width (Dxc) as illustrated in Figure 4. In this study, these two values are normalized by the slope height (H).
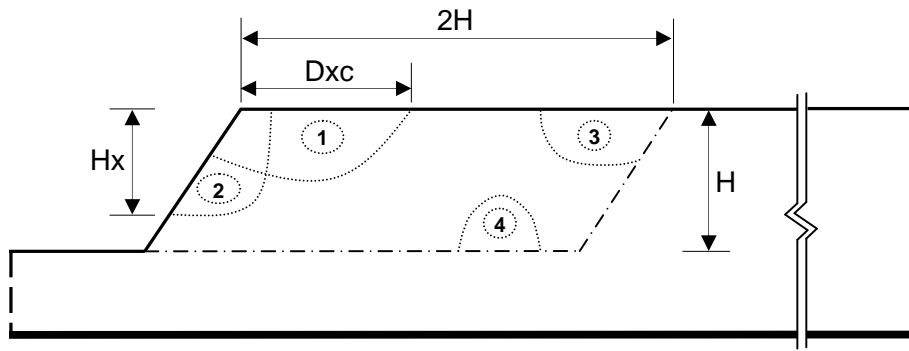


**Figure 4.**     Schematic location of the amplification zones and studied region in a slope model and their corresponding dimensions

## 3   IMPACT OF DIMENSIONLESS FREQUENCY AND GEOMORPHOLOGIC PARAMETERS IN EVALUATING THE SITE EFFECT

The dimensionless frequency ($\eta$) described by formula (6) was used in some research works (De Martin and Kobayashi, 2010; Glinsky and Bertrand, 2011; Messaoudi et al., 2011; Nguyen, 2005; Nguyen and Gatmiri, 2007). As shown in the formula, this parameter integrates several geomorphologic and seismic parameters such as: the slope height (H), the seismic wave frequency (F), the Young's modulus (E), the Poisson's ratio ($\nu$) and the density ($\rho$). This parameter presents therefore a great potential in evaluating and predicting the site effects.

$$\eta = \frac{H}{\lambda} = \frac{H \times F}{V_s} = \frac{H \times F}{\sqrt{\dfrac{E}{2(1+\nu)\rho}}}$$

(6)

### 3.1   Calculation on slope models with constant slope angle

#### 3.1.1   *Slopes with the same value of $\eta$*

According to formula(6), the $\eta$ value depends on five parameters: H, F, E, $\nu$, $\rho$. The question is to know whether the same results in terms of the three interpretation criteria is obtained when the values of these five parameters vary but keeping the value of $\eta$ constant. To answer this question, numerous numerical simulations were performed in slope models having the same slope angle (50°) by varying each time two

of the five parameters, so that the η value is always equal to 0.1. So, there are 10 possible couples of parameters as presented in Table 1. For each couple of parameters, their values were changed 4 times. The coefficient of variation (CV, ratio of the standard deviation to the mean) which represents the dispersion of the result values such as Ax, Ay, $pS_A$, $pS_{AS}$, Hx and Dxc, is calculated for each couple and represented in the Figure 5. The analysis of the obtained results is based on the value of interpretation criteria. Detailed results are presented in (Nguyen and Fleurisson, 2013). In order to have the as best as possible simulation of the seismic wave transmission, the mesh size of the numerical slope model was set as small as possible and also considering the calculation time. For these 40 numerical simulations, the value of N in formula (1) was set to 100.

From a general point of view, the Figure 5 shows that there is dispersion in the calculated results, which means that the amplification factor is not exactly the same even if the dimensionless frequency is constant. It underlines that the specific role of some of the five integrated parameters (H, F, E, ν, ρ) cannot be totally neglected.

In terms of the horizontal amplification factor Ax, a small deviation of about 2.5% is observed for the cases 1 and 2 where the slope height is a varying factor. So, even if the influence is slight, but the value of Ax depends on the slope height.

Concerning the extension of the amplification zone expressed by the two parameters $pS_A$ and $pS_{AS}$, a non null value of the coefficient of variation was found in the three cases: 1 (17%), 2 (17%) and 4 (3%). For all of these cases, one of two varying factors is also the slope height. This indicates that the impact of the slope height is considerable and cannot be neglected. Figure 6 illustrates the spatial distribution and the intensity of the horizontal acceleration amplification in a slope model. The dotted curve represents the isovalue line of the horizontal amplification factor equal to 1.0. The study region $S_T$ is also represented by the zone limited by the slope and the dashed segments. The colours represent the amplification intensity in the slope model. It can be pointed out that the lower the slope height, the higher the horizontal amplification factor and the affected zone area.

Concerning the vertical acceleration amplification Ay, 6 out of the 10 analysed cases show a significant value of coefficient of variation (between 10% and 15%). Cases 1 and 2 correspond to a large variation of the slope height (H), whereas the 4 other cases (3, 6, 8, and 10) concern a change in the value of Poisson's ratio (ν). These results indicate that the Ay value depends on H and on ν.

For the size of the horizontal amplification zone in the surroundings of the slope crest, Figure 5 shows that: the height Hx depends on the slope height, the width Dxc depends on both slope height H and Poisson's ratio ν.
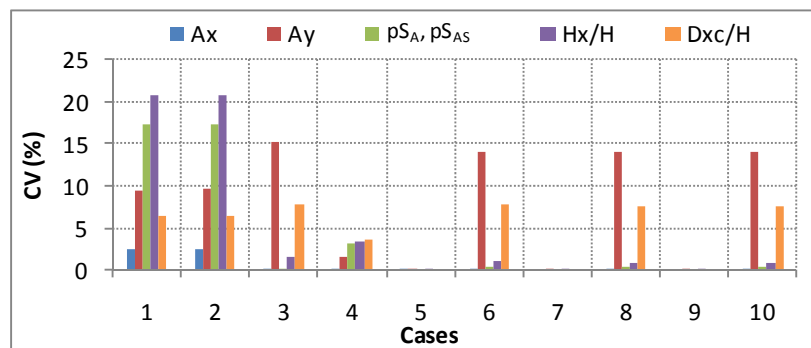


**Figure 5.** Coefficient of variation of numerical simulation results for 10 parametric analyses on slope models with the same value of dimensionless frequency (η=0.1) and the same slope angle (α=50°)

**Table 1.**    Parametric analyses and the corresponding numbering

| Couple of varying parameters | [H,F] | [H,E] | [H,ν] | [H,ρ] | [F,E] | [F,ν] | [F,ρ] | [E,ν] | [E,ρ] | [ν,ρ] |
|---|---|---|---|---|---|---|---|---|---|---|
| Numerical simulation number | 1 | 2 | 3 | 4 | 5 | 6 | 7 | 8 | 9 | 10 |



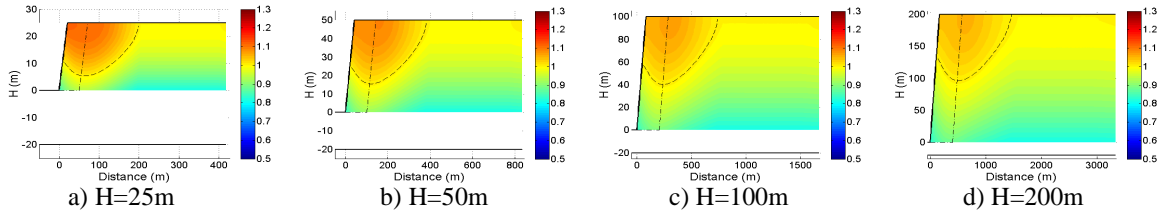a) H=25m          b) H=50m          c) H=100m          d) H=200m

**Figure 6.**    Spatial distribution of the horizontal acceleration amplification for slopes with the same value of dimensionless frequency (η=0.1), the same slope angle (α=50°) but different values of slope height



a) H=25m          b) H=50m          c) H=100m          d) H=200m

**Figure 7.**    Spatial distribution of the vertical acceleration amplification for slopes with the same value of dimensionless frequency (η=0.1), the same slope angle (α=50°) but different values of slope height



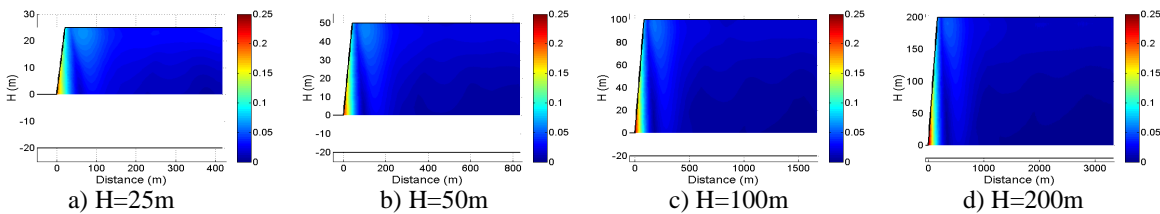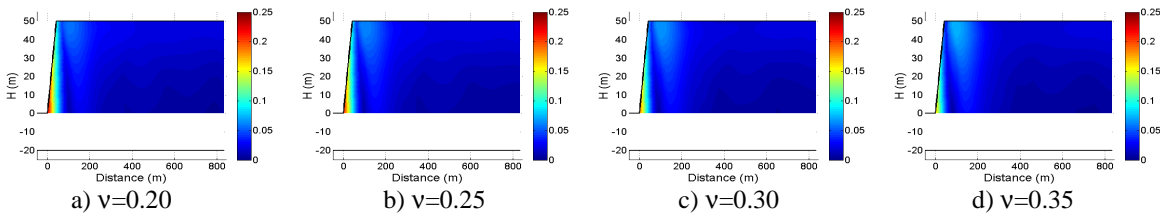a) ν=0.20          b) ν=0.25          c) ν=0.30          d) ν=0.35

**Figure 8.**    Spatial distribution of the vertical acceleration amplification for slopes with the same value of dimensionless frequency (η=0.1), the same slope angle (α=50°) but different values of Poisson's ratio

### 3.1.2  *Slopes with different values of η*

Slope models of the same geomorphological and mechanical characteristics (α=50°, H=40m, E=800MPa, ν=0.25, ρ=2000kg/m3) were subjected to sinusoidal seismic signals of different frequencies (F=0.5÷10Hz), so that the intrinsic η value varies from 0.05 to 1.0. The numerical simulation results are presented in three graphs in Figure 9. The observation of the graph a shows that the value of amplification factors (Ax, Ay) has a global trend to increase with the increase of the value η. On the contrary, the proportion of the horizontal amplified zone area ($pS_A$, $pS_{AS}$), and the dimension of the horizontal amplification zone in the surroundings of the crest (Hx, Dxc) have a tendency to decrease, when the value of η increases (graphs b and c)

Regarding the spatial distribution of horizontal amplification zones, Figure 10 shows that the higher the value of η, the higher the number of amplification zones. From the results of numerous numerical simulations, two thresholds of η are brought out: 0.15 and 0.5.

- η≤0.5: all the amplified zones are located along the free surface, no one appears inside the slope model.
  - η≤0.15: there is only one single amplified zone in the whole slope which located at the crest of the slope model.
  - η>0.15: additional amplified zones appear behind the crest of the slope model.
- η>0.5: amplified zones appear along the free surface and inside the slope model.

Concerning the vertical amplification, the graphs in Figure 11 lead to identify one threshold value of η equal to 0.5.

- η≤0.5: the highest amplified zone is located along the slope.

- η>0.5: the highest amplified zone is located at the crest of the slope.



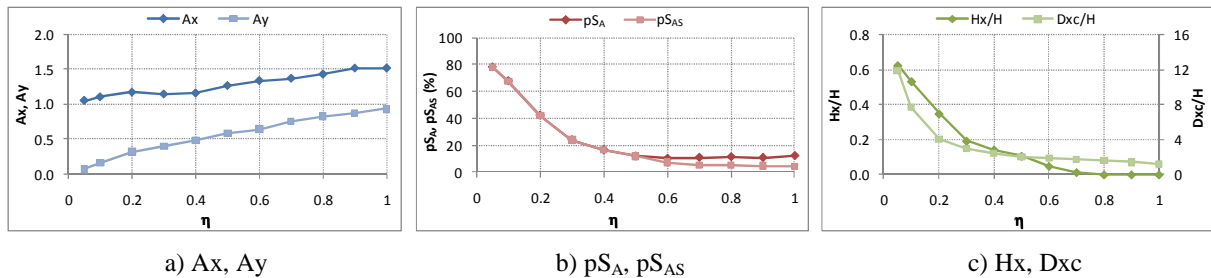a) Ax, Ay          b) pS$_A$, pS$_{AS}$          c) Hx, Dxc

**Figure 9.** Variation of interpretation criteria as a function of the variation of the value of η for slopes with the same value of slope height (H=40m) and the same slope angle (α=50°)



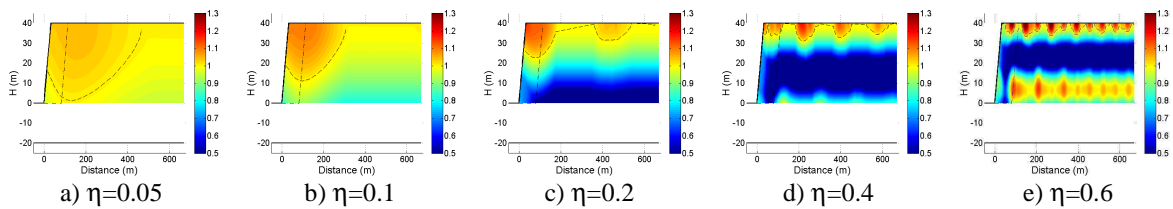a) η=0.05     b) η=0.1     c) η=0.2     d) η=0.4     e) η=0.6

**Figure 10.** Spatial distribution of the horizontal acceleration amplification for slopes with the same value of slope height (H=40m), the same slope angle (α=50°) but different values of dimensionless frequency



a) η=0.05     b) η=0.1     c) η=0.2     d) η=0.4     e) η=0.6
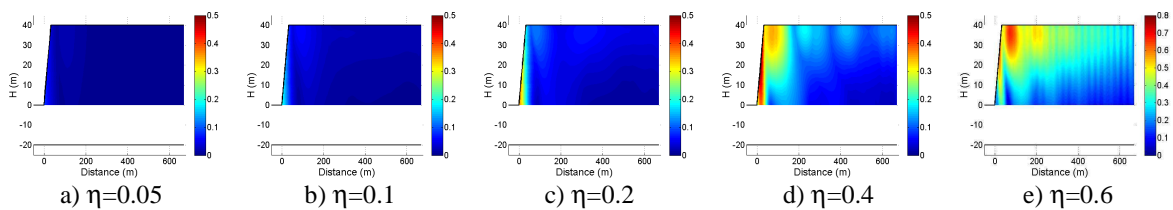
**Figure 11.** Spatial distribution of the vertical acceleration amplification for slopes with the same value of slope height (H=40m), the same slope angle (α=50°) but different values of dimensionless frequency

### 3.2 Calculation on slope models with different slope angles

Slope angle plays an important role not only on the amplification factor, but also on the size of the amplified zone. Different numerical simulations were performed by varying slope angle from 30° to 80° with a step of 10°. The Figure 12 represents the results with value of η ranging between 0.1 and 0.4.

The results presented in the graphs a and b of the Figure 12 confirm again the conclusions of other authors (Di Fiore, 2010; Lenti and Martino, 2012) : the amplification factors (Ax and Ay) increase with an increase in the slope angle.

For the proportion of horizontal amplification zone area ($pS_A$, $pS_{AS}$), the graph c shows that, the relationship between this interpretation criterion and the slope angle depends on the position of the value of $\eta$ regarding the threshold value of 0.15. The value of these parameters increases with an increase in the slope angle when the value of $\eta$ is lower than 0.15, and decreases when the value of $\eta$ is higher than 0.15.

The height of the horizontal amplification zone in the surroundings of the crest (Hx) is dependent on the slope angle when the value of $\eta$ is lower than 0.35: the higher the slope angle, the higher the value of Hx (Figure 12d). But when the value of $\eta$ exceeds this threshold, the role of slope angle is negligible. For the width Dxc, Figure 12e shows that it is independent on the slope angle.



a) Variation of Ax



b) Variation of Ay



c) Variation of $pS_A$, $pS_{AS}$



d) Variation of Hx



e) Variation of Dxc

**Figure 12.** Variation of interpretation criteria as a function of the slope angle $\alpha$ and the value of dimensionless frequency $\eta$ for slopes with the same value of slope height (H=40)

## 4 CONCLUSION

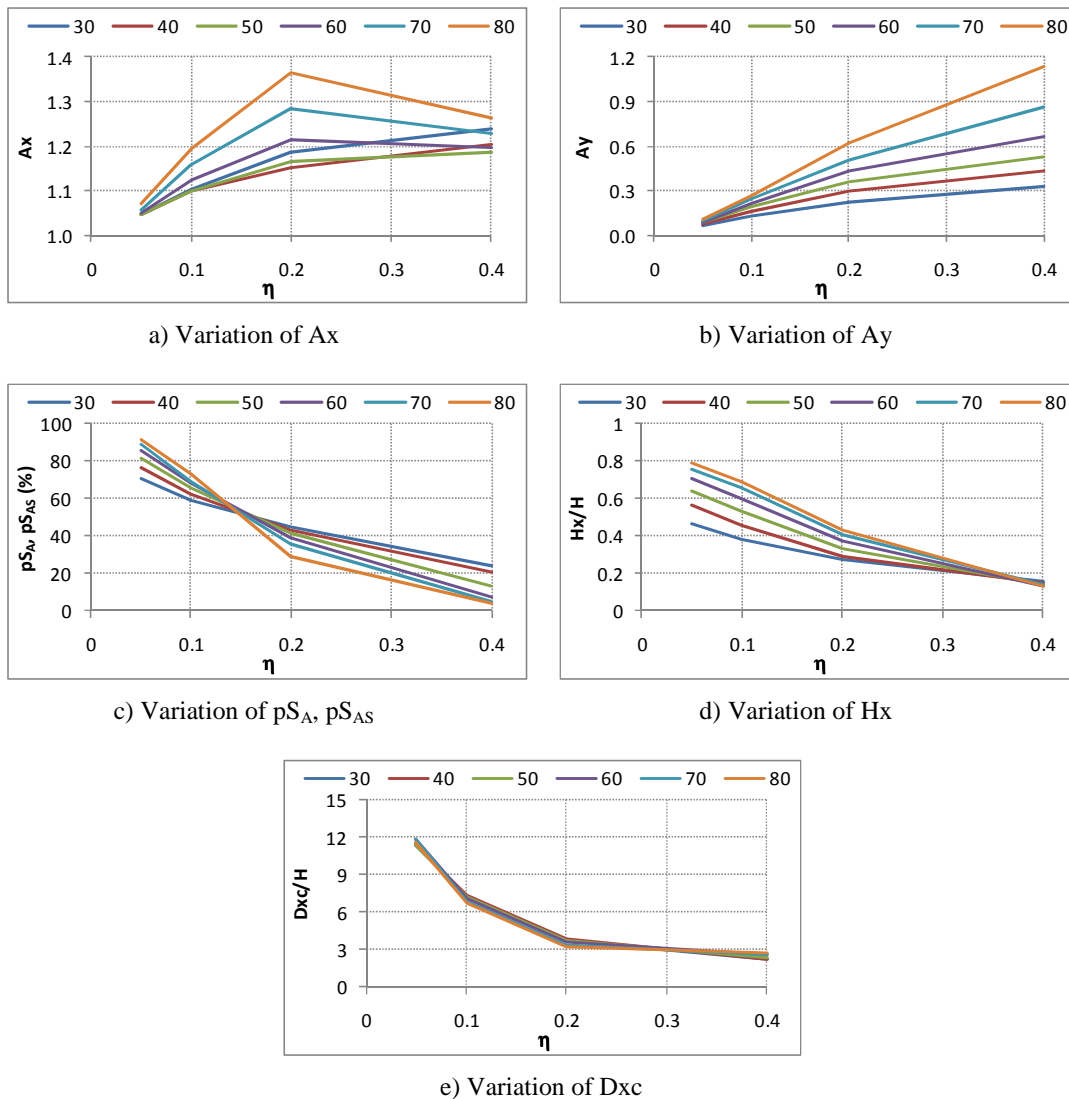This work has focused on the role of the dimensionless frequency ($\eta$). This parameter integrates several geomorphologic and seismic parameters. So, instead of evaluating the topographic site effect under the action of each of these individual factors, $\eta$ can replace them as a pertinent parameter. However, the role of other parameters such as the slope height (H) and Poisson's ratio ($\nu$) cannot be completely neglected, but they play a less important role than $\eta$. Table 2 summarizes the relationships between the interpreting criteria and the parameters which are set in ascending order of importance from the top to the bottom of the table. When the value of a parameter increases, the value of the interpretation criterion can be increased (I), or decreased (D), or non dependent (ND).

In addition, if the slope has relatively simple geomorphologic characteristics and is excited by a real seismic signal with a fairly narrow frequency band, the value of $\eta$ can be calculated by replacing the frequency of the sinusoidal signal by the central frequency of the real seismic signal. So, in this case, the graphs in Figure 12 can be used to estimate the value of Ax, Ay, $pS_A$, $pS_{AS}$, Hx and Dxc.

**Table 2.** Summary table of the relationships between affected factors and interpretation criteria

| | H | $\nu$ | $\alpha$ | $\eta$ |
|---|---|---|---|---|
| **Ax** | D | ND | I | I |
| **Ay** | I ($\eta \leq 0.3$)<br>D ($\eta > 0.3$) | D | I | I<br>$\eta \leq 0.5$: higher amplified zone located along the slope<br>$\eta > 0.5$: higher amplified zone located at the crest |
| **$pS_A$**<br>**$pS_{AS}$** | D ($\eta \leq 0.15$)<br>ND ($\eta > 0.15$) | ND | I ($\eta \leq 0.15$)<br>D ($\eta > 0.15$) | D<br>$\eta \leq 0.5$: amplification zones along the free surface<br>* $\eta \leq 0.15$ : one amplified zone, at crest<br>* $\eta > 0.15$ : many amplified zones<br>$\eta > 0.5$: additional amplification zones inside the slope |
| **Hx** | D ($\eta \leq 0.2$)<br>ND ($\eta > 0.2$) | ND | I ($\eta \leq 0.35$)<br>ND ($\eta > 0.35$) | D |
| **Dxc** | D | I | ND | D |

## 5 PERSPECTIVES

Some perspectives are considered:
  To improve the graphs of Figure 12 by extending the range of value of $\eta$, and by integrating H and $\nu$.
  To develop these graphs for slope having more complex and realistic geomorphologic conditions.
  To develop a calculation method applicable to a real seismic signal with a wide frequency band.

## REFERENCES

Ashford, S. A., Sitar, N., Lysmer, J., and Deng, N. (1997). Topographic effects on the seismic response of steep slopes. *Bulletin of the Seismological Society of America*, vol. **87**: 701-709.

Borcherdt, R. D. (1970). Effects of local geology on ground motion near San Francissco bay. *Bulletin of the Seismological Society of America*, vol. **60**: 29-61.

Bouckovalas, G. D. and Papadimitriou, A. G. (2005). Numerical evaluation of slope topography effects on seismic ground motion. *Soil Dynamics and Earthquake Engineering*, vol. **25**: 547-558.

Bouckovalas, G. D. and Papadimitriou, A. G. (2006). Aggravation of seismic ground motion due to slope topography. *First European Conference on Earthquake Engineering and Seismology.* September 03-08, 2006. Geneva, Switzerland. Paper No: 1171, 10pp.

Bourdeau, C. (2005). *Effets de site et mouvements de versant en zones sismiques : apport de la modélisation numérique.* Ph.D.Thesis defense July 08 2005. Ecole des Mines ParisTech.

Dakoulas, P. (1993). Earth dam-canyon interaction effects for obliquely incident SH waves. *Journal of Geotechnical Engineering*, vol. **119**: 1696-1716.

De Martin, F. and Kobayashi, H. (2010). *Etude des effets d'une topographie sur le mouvement sismique.* Rapport BRGM/RP-59103-FR.

Di Fiore, V. (2010). Seismic site amplification induced by topographic irregularity: Results of a numerical analysis on 2D synthetic models. *Engineering Geology*, vol. **114**: 109-115.

Eurocode 8. (2005). *Calcul des structures pour leur résistance aux séismes. Partie 5: Fondations, ouvrages de soutènement et aspects géotechniques.*

Glinsky, N. and Bertrand, E. (2011). Etude numérique d'effets de site topographiques par une méthode éléments finis discontinus. *8ème Colloque National AFPS 2011-Vers une maîtrise durable du risque sismique.* September 06-08, 2011. Paris, France. p.723-732.

Lenti, L. and Martino, S. (2012). The interaction of seismic waves with step-like slopes and its influence on landslide movements. *Engineering Geology*, vol. **126**: 19-36.

Messaoudi, A., Laouami, N., and Mezouer, N. (2011). Effet de la topographie des pentes sur les réponses sismiques. *8ème Colloque National AFPS 2011-Vers une maîtrise durable du risque sismique.* September 06-08, 2011. Paris, France. p.285-294.

Nguyen, H. T. and Fleurisson, J.-A. (2013). Rôle du paramètre "fréquence adimensionnelle" dans l'évaluation de l'effet de site topographique en cas de séisme. *Conférence Franco-Vietnamienne CIGOS 2013 - Construction et développement durable.* April 04-05, 2013. Lyon, France. Paper No: CIGOS206, 8pp.

Nguyen, V. K. (2005). *Étude des effets de site dus aux conditions topographiques et géotechniques par une méthode hybride éléments finis/éléments frontières.* Ph.D. thesis defense January 17 2005. Ecole des Ponts ParisTech.

Nguyen, V. K. and Gatmiri, B. (2007). Evaluation of seismic ground motion induced by topographic irregularity. *Soil Dynamics and Earthquake Engineering*, vol. **27**: 183-188.

Vanbrabant, F. (1998). *Prise en compte des effets de site topographiques dans l'étude de la stabilité des pentes soumises à des sollicitations dynamiques.* Ph.D. thesis defense November 23 1998. Ecole des Mines ParisTech.